in the ratio of eq 4 become greatly magnified when it is combined with k_1/k_3 to calculate k_1/k_2.

On the other hand, eq 4 *can* be used to calculate precise values of k_1/k_3 if k_1/k_2 is known. We have previously demonstrated that precise k_H/k_T values for substrates with a single reactive hydrogen can be obtained if the molar activity of the product containing the hydrogen (or tritium) abstracted from the substrate is determined after a known extent of partial reaction.[10] The situation is a little more complex with the system of eq 1-3, but it can be shown that eq 5 holds for low extents of reaction, where R_0 is the

$$k_1/k_2 = \tfrac{1}{2}R_0/R^0_{BH} \quad (5)$$

molar activity of the original substrate (RH_2) and R^0_{BH} is the molar activity of BH.[9] The extents of reaction over which eq 5 applies are not impractically low; when F_H = 0.05 (5%), R^0_{BH} is only 1-1.5% larger than its limiting value (as $F_H \rightarrow 0$) for reasonable values of k_1/k_2 and k_1/k_3. These relations (eq 4 and 5) can easily be generalized to any number of equivalent tracer-labeled positions.[9]

We have tested this approach on the bimolecular elimination reaction of (2-phenylethyl-2-*t*)trimethylammonium bromide (1-Br, 8.98 μCi mmol^{-1}) with ethoxide ion in ethanol to yield styrene. The fraction of reaction, F_H, was determined spectrophotometrically, and the reactant was reisolated as the tetraphenylborate (1-BPh_4) after 37-72% reaction. In separate runs, the reaction was stopped at 2.8-5.2% reaction by using insufficient base, the product styrene converted to the dibromide with a little bromine in ethanol, and a portion of the ethanol distilled on a vacuum line (shown previously[10] to occur without isotopic fractionation). Activities were determined by liquid scintillation counting with quench corrections by the external standard channels ratio method.[11] The molar activity of that portion of the ethanol produced in the elimination reaction can be calculated from the observed activity, the initial concentration of substrate, and the fraction of reaction. The statistical precision of the counting was ±0.3% or better.

Three determinations of k_1/k_2 gave values of 4.299, 4.040, and 3.863 for an average of 4.067 ± 0.127 (standard deviation of the mean). Three separate runs gave $2k_1/(k_2 + k_3)$ values of 1.985, 1.988, and 1.975 for an average of 1.983 ± 0.004. Combining these two results gave k_1/k_3 values of 1.313, 1.316, and 1.304. The average is 1.311 ± 0.014. In this case the quoted deviation reflects the combined uncertainties in k_1/k_2 and $2k_1/(k_2 + k_3)$, rather than the unrealistically low figure of 0.004 which would result from simply using the deviations from the mean of k_1/k_3 itself.

The secondary tritium isotopic effect is of the same order as those previously reported for eliminations from quaternary ammonium salts (1.15-1.33 at temperature of 22-130 °C).[6] A $(k_H/k_T)_{sec}$ of 1.311 corresponds to $(k_H/k_D)_{sec}$ of 1.207, using the known relationship between tritium and deuterium isotope effects.[12] Similarly, $(k_H/k_T)_{prim}$ of 4.067 corresponds to $(k_H/k_D)_{prim}$ of 2.649. Directly measured isotope effects on (2-phenylethyl-2,2-d_2)trimethylammonium ion should correspond to the product of the primary and secondary effects, 2.649 × 1.207 = 3.20. This number may be compared to 3.23 measured at 40 °C by Smith and Bourns,[13] and 3.12 calculated from the Arrhenius parameters determined by Kaldor and Saunders.[14]

We are exploring the scope and utility of this method. Detailed mechanistic discussion of the present results seems inadvisable until more data are available for comparison, so we merely point out the main advantages of our approach. Interpretations of pure primary isotope effects should rest on much firmer ground than interpretations of the composite primary and secondary effects usually measured. Precise values of the secondary isotope effects are potentially very useful as an additional measure of the changes in bonding occurring between reactant and transition state, for they might be expected to reflect the extent of rehybridization from sp^3 to sp^2 at the β-carbon atom.

(10) Kaldor, S. B.; Fredenburg, M. E.; Saunders, W. H., Jr. *J. Am. Chem. Soc.* **1980**, *102*, 6296-9.
(11) Neame, K. D.; Homewood, C. A. "Liquid Scintillation Counting"; Wiley-Halsted: New York, 1974; pp 106-10.
(12) Reference 9, p 29.
(13) Smith, P. J.; Bourns, A. N. *Can. J. Chem.* **1974**, *52*, 749-60.
(14) Kaldor, S. B.; Saunders, W. H., Jr. *J. Am. Chem. Soc.* **1979**, *101*, 7594-9.

Single-Collision Gas-Surface Vibrational Energy Transfer in a Reacting System

D. F. Kelley, T. Kasai, and B. S. Rabinovitch*

Department of Chemistry BG-10, University of Washington, Seattle, Washington 98195 *(Received: February 18, 1981)*

Gas-surface vibrational energy accommodation in a reactive system has been studied under single-collision conditions. The reaction system is the isomerization of cyclobutene to 1,3-butadiene. Both seasoned pyrex and silica surfaces were used over the temperature ranges 400-775 and 500-975 K, respectively. Strong collider behavior was observed below ~425 K. The vibrational energy accommodation coefficient was found to decrease with rise of temperature from ~1.0 to 0.2, while the relative collisional efficiency β_1 declined from ~1.0 to 0.008. A stochastic model was used to fit the data.

Introduction

Gas-surface vibrational energy accommodation has been a subject of considerable interest both experimentally and theoretically.[1,2] However, to this time there have been no single-collision measurements of gas-surface energy transfer in a high-temperature reactive system.[3] In the

(1) (a) F. O. Goodman, *Prog. Surf. Sci.*, **5**, 261 (1974); (b) F. O. Goodman and H. Y. Wachman, "Dynamics of Gas Surface Scattering", Academic Press, New York, 1976.
(2) C. W. Draper and G. M. Rosenblatt, *J. Chem. Phys.*, **69**, 1465 (1978).
(3) Single collision studies on cyclopropane, for example, G. Prada-Silva, O. Löffler, B. L. Halpern, G. L. Haller, and J. B. Fenn, *Surface Sci.* **83**, 453 (1979), involved surface catalysis rather than simple energy transfer.

0022-3654/81/2085-1100$01.25/0

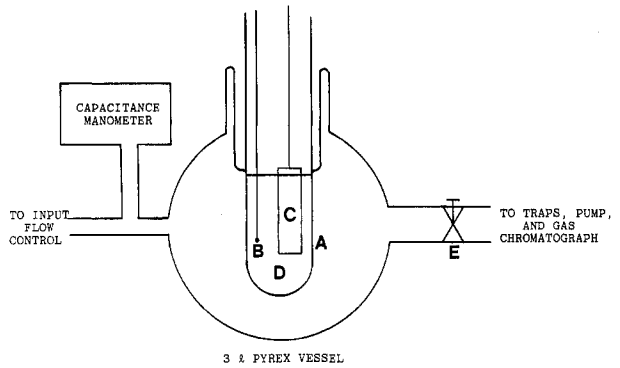

Figure 1. Schematic of single-collision VEM reactor. Shown are pyrex (or silica) reactor finger, A; moveable chromel–alumel thermocouple, B; heaters, C, in two sections, top and bottom; eutectic bath, D; and variable flow stopcock, E.

present communication, we describe the application of the variable encounter method (VEM)[4-8] to the study of single-collision measurements with seasoned heated glass surfaces. Although such a surface is not well defined, it is the conventional experimental surface of thermal unimolecular kinetics.

The VEM technique has previously been applied to the study of energy transients: molecules are thermally equilibrated at some low temperature before experiencing an encounter, i.e., a sequence of m collisions (where m is variable and is chosen to be 1 in the present study) with a hot reactor surface; after the encounter, unreacted molecules are reequilibrated at the original low temperature. The amount of gas-phase unimolecular reaction that occurs following surface activation gives the fraction of those molecules in the original Boltzmann distribution N_c that have been transported to energy levels above the critical reaction threshold, E_0. As m increases, N_c approaches N_{ss}, the steady-state population distribution characteristic of reactive depletion at the reactor temperature.

In the present work, the hot surface is convex, ensuring that only a single collision occurs on encounter of the molecule with the surface. The single-collision case has the advantage over previous multicollision VEM work (where $m = \sum_{n=1}^{\infty} nf(n)$), in that no averaging over some normalized distribution $f(n)$ of numbers of collisions made by the molecule per encounter with the reactor is necessary in the deconvolution of the data. This provides greater experimental stringency and constraints on suitable models for the collisional transition probability matrix, **P**. The present study also permits a more direct evaluation of the gas–surface vibrational energy accommodation coefficient, α.

The ring-opening unimolecular isomerization of cyclobutene to 1,3-butadiene has a low[9] E_0 (32.4 kcal mol^{-1}) and is substantially in the low-pressure region at typical experimental pressures, 1×10^{-4} to 5×10^{-4} torr. The reaction proceeds with no indication of surface catalysis.[7,8] On the basis of the increasing strength of collision with decreasing temperature that was observed in earlier VEM studies, these characteristics make this species suitable for single-collision study, and a significant amount of reaction should occur at lower temperatures.

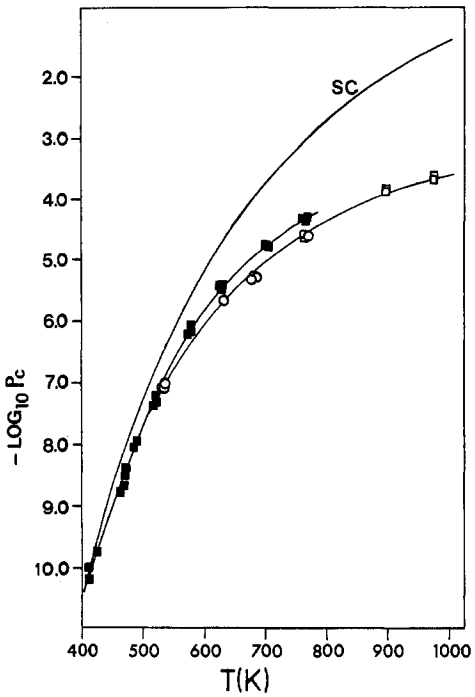

Figure 2. Plots of experimental values of P_c vs. T for the following reactors and conditions: pyrex, static (■); silica, static (○); and silica, flow (□). Also shown is a calculated strong-collider (sc) curve. The magnitudes of random errors are approximately given by the size of the symbols. The magnitude of unspecified systematic errors may be judged from the scatter of the data; such errors are largest at low temperatures and are believed to be primarily due to error in temperature (see text).

Experimental Section

The reactant cyclobutene was 99.9% pure. The reactor is shown schematically in Figure 1. The reaction vessel consisted of a 3-L pyrex flask with an internally heated, central reactor finger, A. Two different reaction vessels were used, fitted with pyrex and silica reaction fingers, respectively. The vessel wall was cooled by an ice bath. Liquid Bi–Pb–Sn eutectic was used as the internal bath medium (D) in the reactor finger and the top and bottom regions were heated independently (C) to minimize axial temperature variations. At the highest temperature (970 K) the maximum deviation was ±5 °C and was significantly less at lower temperatures. Temperature measurements were made with calibrated chromel–alumel thermocouples (B). Before kinetic measurements were made, the reactor was "seasoned" at 750 K by preexposure for several hours to cyclobutene at a pressure of $\sim 5 \times 10^{-3}$ torr.

The system was run in both static and flow modes. In the former, the reactor was pumped to $<10^{-6}$ torr and substrate was admitted at a pressure between 10^{-4} and 10^{-3} torr. The gas was pumped out and analyzed after a predetermined run time. For flow-mode runs, the impedance of a variable exit control valve was calibrated by pressure-drop measurements. A substrate entry flow control provided gas delivery rates of 2.5×10^{-2} to 0.22 torr cm^3 s^{-1}. Typical residence times were 10 to 100 s, and pressure rose from $<10^{-6}$ to $<10^{-3}$ torr during a run, which was terminated by closing the variable flow stopcock after about 30 to 60 s. Pressure measurements were made with an MKS Model 170 capacitance manometer.

(4) D. F. Kelley, L. Zalotai, and B. S. Rabinovitch, *Chem. Phys.*, **46**, 379 (1980).
(5) M. C. Flowers, F. C. Wolters, B. D. Barton, and B. S. Rabinovitch, *Chem. Phys.*, **47**, 189 (1980).
(6) D. F. Kelley, T. Kasai, and B. S. Rabinovitch, *J. Chem. Phys.*, **73**, 5611 (1980).
(7) M. C. Flowers, F. C. Wolters, D. F. Kelley, and B. S. Rabinovitch, *Chem. Phys. Lett.*, **69**, 543 (1980).
(8) F. C. Wolters, M. C. Flowers, and B. S. Rabinovitch, *J. Phys. Chem.*, **85**, 589 (1981).
(9) C. S. Elliott and H. M. Frey, *Trans. Faraday Soc.*, **62**, 895 (1966).

Product analysis was performed by gas–liquid chromatography on a 5 ft × 3/16 in. squalane column at 0 °C with FID.

Results and Discussion

The probability of reaction per collision, P_c, was calculated from the product yield in both static and flow (Appendix) cases, and is plotted as a function of temperature in Figure 2. Uncertainties in P_c varied from about ±7% at the highest to ±20% at the lowest temperatures. This is due to the greater temperature sensitivity at the lower temperatures. Also shown is a strong collider curve, calculated on the basis of the vibration frequency assignments of Elliott and Frey.[9] The experimental curves coalesce at lower temperature where strong collider behavior is approached. At higher temperatures, slightly larger reaction probabilities were obtained with the pyrex reactor finger. Although the difference between the experimental curves is small, it exceeds the experimental uncertainty at the higher temperatures, and appears to represent either a minor difference in the rate of energy transfer on the pyrex-based vs. silica-based surfaces or, possibly, a small difference in the preparation and seasoning procedures for the two fingers.

The mathematical models usually used to interpret energy transfer data both in conventional thermal[10] and VEM[4] systems give the probability, $P(\Delta E)$, of a down transition of magnitude ΔE by the substrate molecule as an exponential (eq 1) or Gaussian (eq 2) function, where

$$P(\Delta E) = c_1 \exp(-\Delta E/\langle \Delta E \rangle) \quad (1)$$

$$P(\Delta E) = c_2 \exp(-(\Delta E - \Delta E_{mp})^2/2\sigma^2) \quad (2)$$

$\langle \Delta E \rangle$, ΔE_{mp} and σ are adjustable parameters and the c's are constants. These functions, along with the detailed balance and completeness relations, specify **P**.[11] However, these forms are inadequate to describe near-strong collider behavior. As strong collider behavior is approached, the columns of **P** should approach normalized Boltzmann vectors **B** characteristic of the reactor temperature, T_r, i.e., $P_{i\leftarrow j} = B_i$, for all i, j; this condition is clearly not met by eq 1 or 2. All choices of parameters with these models give values of P_c that are significantly below strong collider and the present observed values. The Boltzmann-weighted exponential (BE, eq 3) does fit the data and gives the

$$p_{i\leftarrow j} = c_3 \exp(-\Delta E/\langle \Delta E \rangle) g_i \exp(-E_i/kT_r) \quad (3)$$

correct strong collider limiting behavior; here g_i is the density of vibrational states at level E_i, and c_3 is a constant.

The calculated average amount of energy $\langle \Delta E' \rangle_{E_0}$ transferred in a down step from hot molecules at the level of energy E_0 is shown in Table I for several reactor temperatures. Still another quantity of interest is the average energy transfer, ΔE_{av}, defined as the difference in average energies of substrate molecules before, $\bar{E}_i$, and after, $\bar{E}_f$, collision; $\bar{E}_i$ refers to the flask temperature (273 K). This is related to the vibrational accommodation coefficient $\alpha = \Delta E_{av}/(\bar{E}_r - \bar{E}_i)$, where $\bar{E}_r$ is the average energy of substrate molecules at the reactor finger temperature. Values of α and of ΔE_{av} are given in Table I. Also given are values of the collisional efficiency β_1, defined as $\beta_1 = P_c/P(sc)$, as well as efficiencies β_{ss} that would be observed in an equivalent steady-state thermal system; $\beta_{ss} = P(\infty)/P(sc)$, where $P(\infty)$ is the actual steady-state reaction probability per collision and $P(sc)$ is the strong-collider value of the reaction probbility per collision. β_{ss} is the same value that would apply in a low-pressure gas-phase thermal unimolecular system where it is defined as $\beta_{ss} = k_0^{wc}/k_0^{sc}$; $\omega^{wc} = \omega^{sc}$; or equivalently as $\beta_{ss} = \omega^{sc}/\omega^{wc}$, $k_0^{wc} = k_0^{sc}$; here k_0^{wc} and k_0^{sc} are the observed low-pressure rate constants measured at constant collision frequencies ω^{wc} and ω^{sc} in a weak-collider and strong-collider system, respectively. It is evident from Table I that since the β_{ss} values group close to unity at all temperatures, a less stringent test of energy transfer behavior is available in steady-state experiments as compared to the present measurements of β_1 in the transient region. In reactive systems, β_1 is also a more sensitive function of energy transfer efficiency than is α, since the former tests efficiency relative to the difference, $E_0 - \bar{E}_i$, while the latter tests efficiency relative to the difference, $\bar{E}_r - \bar{E}_i$.

TABLE I: Energy Transfer Parameters in the Cyclobutene System[a]

	T, K					
	400[b]	500	600	750	875	975
$\langle \Delta E' \rangle_{E_0}$, cm^{-1}	10550	8940	6925 (7520)	4200 (4700)	3125	2540
ΔE_{av}, cm^{-1}	465	720	780 (900)	900 (1000)	1050	1135
α	1.0	0.57	0.40 (0.47)	0.28 (0.31)	0.23	0.20
β_{ss}	1.0	1.0	0.994 (0.998)	0.87 (0.92)	0.68	0.51
β_1	1.0	0.40	0.14 (0.22)	0.029 (0.048)	0.0134	0.008

[a] Parenthetic values apply to the pyrex reactor. Pyrex and silica reactors give indistinguishable results at 500 K. [b] Strong-collider behavior.

The decline in collisional efficiency that occurs with rise of temperature in Figure 2 and Table I has been observed previously in cyclobutene VEM studies[7,8] where strong collider behavior was inferred below ~450 K, as has been found here. This same general trend has been observed in all VEM studies and in conventional homogeneous thermal studies at higher temperatures. It is also generally observed in energy accommodation studies.[1] This trend appears to be related to the fact that as the temperature is lowered the time that the molecule spends trapped in the gas–surface potential well increases. The Boltzmann-weighted models then correspond more closely to the case of statistical accommodation on the surface, with relaxation of the restrictions on conservation of angular momentum that apply in gas–gas systems.[12]

Draper and Rosenblatt measured vibrational energy accommodation coefficients of hydrocarbons on metal surfaces at room temperature by a vibrating diaphragm technique.[2] Although those experiments are not directly comparable to ours, we note that their values of α_{vib} are fairly close to unity, i.e., 0.7 to 0.8. For larger molecules, i.e., as the depth of the potential well increased, they found that the values of α_{vib} also increased.

One final comment: the present data on energy transfer efficiency extend upward from 425 K; the low temperature region from ~200 to ~700 K is one that has previously been explored in thermal, chemical activation, and photoexcitation reactive systems with conflicting conclusions as to whether efficiency increases or decreases with rise of temperature.[10] The present system reveals marked decrease in $\langle \Delta E' \rangle$, β_1, and α in this region with rise of temperature.

(10) D. C. Tardy and B. S. Rabinovitch, *Chem. Rev.*, **77**, 369 (1977).
(11) D. C. Tardy and B. S. Rabinovitch, *J. Chem. Phys.*, **45**, 3720 (1966).
(12) Y. N. Lin and B. S. Rabinovitch, *J. Phys. Chem.*, **74**, 3151 (1970).

Appendix. Flow System: Apparent Rate Constant

Mass conservation requires

$$V\frac{dR}{dt} = Q' - F'R - kVR \qquad V\frac{dP}{dt} = -F'P + kVR$$

where $R(t)$ and $P(t)$ are the concentrations of reactants and products at time t, respectively; Q' is the flux of reactant into the reaction vessel of volume V; k is the apparent rate constant ($= P_c\bar{c}A/4V$, where $\bar{c}$ is the mean molecular speed and A is the heated reactor area); and F' is the Knudsen output flow impedance. Since the reactor in initially evacuated, $P(0) = 0$, $R(0) = 0$. The amount of product collected, P_T, is given by

$$P_T = F'\int_0^{t_m} P(t)\,dt$$

where t_m is the run time. An analogous expression applies for the amount of reactant collected R_T. One obtains

$$\frac{R_T}{R_T + P_T} = \frac{F}{F+k}\,\frac{t_m - \frac{1}{F+k}[1 - \exp(-(F+k)t_m)]}{t_m - \frac{1}{F}[1 - \exp(-Ft_m)]}$$

where $F = F'/V$. This equation may be solved iteratively for k.

Acknowledgment. This work was supported by the Office of Naval Research.

Oscillatory Oxygen Evolution during Catalyzed Disproportionation of Hydrogen Peroxide[1]

N. Ganapathisubramanian and Richard M. Noyes*

Department of Chemistry, University of Oregon, Eugene, Oregon 97403 *(Received: February 20, 1981)*

If heterogeneous effects are reduced by hydrophic coating of glass surfaces, variations are observed in the rate of gas evolution during iron sulfate catalyzed disproportionation of aqueous hydrogen peroxide. Amplitudes of these variations may be over 20% of the mean rate with periods of the order of 1 min. Several bubbles per second are escaping, and these variations in rate cannot be statistical fluctuations. Chemical and thermokinetic instabilities are also rejected. The effect is ascribed to the finite lag time between nucleation and escape of bubbles.

Pulsed evolution of gas has been reported for the dehydration of formic acid by sulfuric acid,[2,3] for its oxidation by mixed nitric and sulfuric acids,[4] and for the decomposition of aqueous ammonium nitrite.[5] However, most other reactions that produce dissolved gas continuously have been assumed to be accompanied by nonperiodic evolution of that gas. That assumption has been put in question by the recent observation of Bowers and Dick[6] that decomposition of aqueous benzene diazonium salts included an oscillatory component with a period of about 5 s.

Another well-known reaction that generates gas is the disproportionation of aqueous hydrogen peroxide catalyzed by iron salts. Although this system has been studied for a long time, we have not found any reference to oscillatory gas evolution.

The experiments reported here were conducted in a closed 200-mL flask about half full of solution and fitted with a capillary leak consisting of 23 cm of 0.5-mm diameter glass tubing. Pressure in the flask was monitored with a Pace-Wianko variable reluctance differential pressure transducer connected through a transducer indicator to a conventional recorder. If no hydrogen peroxide was present, excess air injected into the flask decayed by leakage with a time constant of about 0.85 min^{-1}.

Initial observations were discouraging. Pressure in the flask exhibited noisy small-amplitude fluctuations without any detectable periodic component. Examination of the system indicated at least a major fraction of the bubbles was originating on the glass surface of the flask.

Various types of hydrophobic coatings were tried, and the most successful employed dichlorodimethylsilane, $(CH_3)_2SiCl_2$. Although heterogeneous decomposition was by no means eliminated, the fraction of the surface covered by bubbles at any time was considerably reduced by this coating.

Figure 1 shows a pressure trace when the catalyst was initially ferric iron. The initial slowly accelerating increase in pressure was presumably due to effects of gas solution and escape or to a modification of the flask surface rather than to autocatalytic chemical change. After about 7 min of slow increase, the excess pressure in the flask began to fluctuate with an amplitude of over 20% and a period of the order of 1 min. Visual observation confirmed that several bubbles were escaping from the solution each second, and the much longer time scale of the effects in Figure 1 demonstrates we are not looking at purely statistical fluctuations in the rate of escape of bubbles. We conclude that the rate of bubble nucleation is undergoing significant variations. The observations reported here do not establish whether the affected nucleation rate is homogeneous or heterogeneous, but we do not see how the

(1) Part 43 in the series "Chemical Oscillations and Instabilities". Part 42: Noyes, R. M.; Furrow, S. D. *J. Am. Chem. Soc.* Submitted for publication.
(2) Morgan, J. S. *J. Chem. Soc.* **1916**, *109*, 274–283.
(3) Showalter, K.; Noyes, R. M. *J. Am. Chem. Soc.* **1978**, *100*, 1042–1049.
(4) Raw, C. J. G.; Frierdich, J.; Perrino, F.; Jex, G. *J. Phys. Chem.* **1978**, *82*, 1952–1953.
(5) Degn, H. Informal report at European Molecular Biology Organization Workshop, Dortmund; Oct 4–6, 1976.
(6) Bowers, P. G.; Dick, Y. M. *J. Phys. Chem.* **1980**, *84*, 2498.

0022-3654/81/2085-1103$01.25/0